Pergamon

Int. J. Heat Mass Transfer. Vol. 38, No. 18, pp. 3359–3367, 1995

0017–9310/95 $9.50+0.00

0017–9310(95)00101–8

Integral transform methodology for convection–diffusion problems in petroleum reservoir engineering

ALCINO RESENDE ALMEIDA
Petrobras Petróleo Brasileiro S/A, CENPES/DIPLOT, Ilha do Fundão Quadra 7, Rio de Janeiro, RJ-21949-900, Brazil

and

RENATO MACHADO COTTA†
Mechanical Engineering Department, EE/COPPE/UFRJ, Universidade Federal do Rio de Janeiro, Cx.Postal 68503, Rio de Janeiro, RJ-21945-970, Brazil

(*Received* 5 *August* 1994 *and in final form* 17 *February* 1995)

Abstract—The convection–diffusion equation is present in the formulation of many petroleum reservoir engineering problems. A representative example, the tracer injection problem, is solved analytically here, through the generalized integral transform technique so as to illustrate the usefulness of this approach, for this class of problems. Classical assumptions, such as steady-state single phase flow and unit mobility ratio, are adopted. Comparisons with alternative analytical (when available) or numerical (finite difference) solutions are performed and benchmark results are established.

INTRODUCTION

Various physical situations of engineering interest are modelled by means of the convection–diffusion equation. Approximate analytical or purely numerical approaches are frequently used to solve this equation, since the conventional analytical methods may be employed only in very simple cases. However, the ideas in the so-called generalized integral transform technique (GITT) [1] can be used to develop analytical or hybrid (numerical–analytical with prescribed accuracy, i.e. computationally exact) solutions for both benchmark purposes and direct engineering application. Convection–diffusion problems have already been treated through the GITT for one-dimensional transient formulations (viscous linear and non-linear Burgers' equation) and multidimensional steady-state applications [2–4]. These exploratory studies were aimed at increasing the knowledge basis for more involved applications like the one to be discussed here.

In petroleum reservoir engineering many phenomena are governed by the convection–diffusion equation and one of the most representative problems is that related to tracer transport. Tracers have been injected in underground porous media since the beginning of this century in order to extract qualitative information about flow barriers, directional flow trends, communication between reservoirs, and so on. However, it is possible to extract quantitative information if one has an adequate model of the tracer transport and the features of the reservoir, and a reliable way of solving it.

Tracer transport in a petroleum reservoir is basically subjected to convection (bulk movement of fluids caused mainly by the injection and the production wells) and mechanical dispersion along the main flow direction (longitudinal mixing) [5, 6]. This leads to the use of the convection–diffusion (dispersion) equation and, depending upon the ratio of convective to diffusive (dispersive) contributions to tracer transport, its behavior ranges from parabolic to almost hyperbolic, and such a wide range of practical situations brings up a serious difficulty in the application of purely numerical methods.

In this first application of the GITT in petroleum reservoir problems, the two-dimensional tracer equation is solved for a fully developed five-spot pattern, i.e. an infinite array of injection and production wells arranged as shown in Fig. 1. From symmetry considerations one can observe that the five-spot pattern may be reproduced by the repetition of a single cell. For the present purposes, a convenient choice of such a cell is illustrated in Fig. 1, with the associated coordinate system. Classical assumptions are adopted, including horizontal, homogeneous and isotropic reservoir, incompressible single phase steady-state flow, unit mobility ratio and ideal tracer (no adsorption, chemical reaction or radioactive decay).

† Author to whom correspondence should be addressed.

NOMENCLATURE

a	distance between like wells [m]
$\mathbf{B}$	coefficients matrix of the ordinary differential equations (ODE) system [s^{-1}]
C	concentration [kg m^{-3}]
C_1	concentration of species one [kg m^{-3}]
C_{1s}	concentration of species one for the slug injection problem [kg m^{-3}]
$\bar{C}_{im}$	transformed potential (concentration) associated with the ith eigenvalue in the x direction, and with the mth eigenvalue in the y direction [kg m^{-3}]
C_{inj}	injection concentration [kg m^{-3}]
C_m	average potential (concentration) over the whole domain [kg m^{-3}]
C_N	normalized concentration [dimensionless]
C_p	steady-state solution of the concentration equation [kg m^{-3}]
C_{prod}	concentration at the production wells [kg m^{-3}]
C_t	transient solution of the concentration equation after extraction of steady-state solution [kg m^{-3}]
d	distance between unlike wells [m]
f_{VP}	tracer slug volume, fraction of pore volume
h	reservoir thickness [m]
k	permeability [m^2]
$\mathbf{K}$	dispersion–diffusion tensor [$m^2 s^{-1}$]
M_m	mth norm in the y direction [m]
N_i	ith norm in the x direction [m]
p	pressure [Pa]
Pe	Peclet number ($= a/\alpha$) [dimensionless]
q	injection or production rate into the five-spot unit (one-quarter of the total well rate) [$m^3 s^{-1}$]
Q	source term, in the continuity equation, corresponding to the wells [s^{-1}]
t_{inj}	injection time [s]
$\mathbf{u}$	Darcy's velocity [m s^{-1}]
u_0	characteristic (Darcy's) velocity [m s^{-1}]
u_x	Darcy's velocity component in the x direction [m s^{-1}]
u_y	Darcy's velocity component in the y direction [m s^{-1}].

Greek symbols

α	dispersivity [m]
$\delta(\ldots)$	Dirac's delta function [m^{-1}]
δ_{ik}	Kronecker's delta
$\zeta^{(l)}$	lth eigenvector of matrix $\mathbf{B}$ [s]
λ_m	mth eigenvalue in the y direction [m^{-2}]
μ	viscosity [Pa s]
μ_i	ith eigenvalue in the x direction [m^{-2}]
ν_l	lth eigenvalue of matrix $\mathbf{B}$ [s^{-1}]
σ_l	lth coefficient in the linear combination of elementary solutions of the ODE system (21) [kg $m^{-3} s^{-1}$]
φ_m	mth eigenfunction in the y direction [dimensionless]
Φ	porosity [dimensionless]
ψ_i	ith eigenfunction in the x direction [dimensionless].

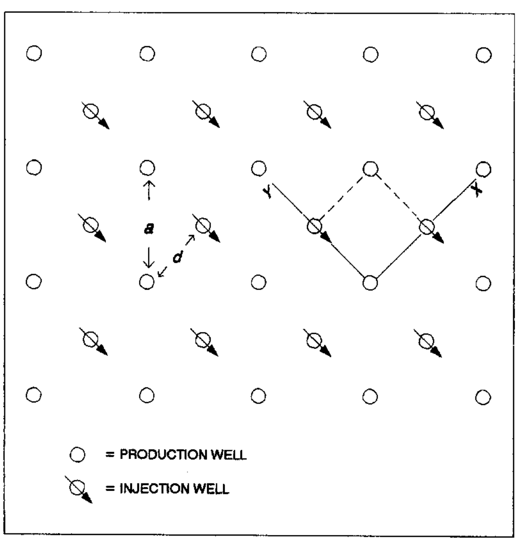

Fig. 1. Geometry and coordinate system for the five-spot pattern.

PROBLEM FORMULATION

Flow field

Since the tracer transport phenomena depend upon the velocity field imposed by the injection and production wells, it is then necessary to determine such a flow field *a priori*, recalling that this is a steady-state flow system.

For the present case, the continuity equation may be expressed as:

$$\nabla \cdot \mathbf{u} = Q(x, y) \quad (1)$$

where $Q(x, y)$ takes into account the sources (injection wells) and the sinks (production wells). Assuming that the wells can be reduced to line sources/sinks and using the cell and coordinate system presented in Fig. 1, one obtains [7]:

$$Q(x,y) = \frac{q}{h}[\delta(x)\delta(y-d) + \delta(x-d)\delta(y) - \delta(x)\delta(y) - \delta(x-d)\delta(y-d)]. \quad (2)$$

Darcy's law relates velocity and pressure fields as follows:

$$\mathbf{u} = -\frac{k}{\mu}\nabla p. \tag{3}$$

Therefore, combining equation (1)–(3), one finds:

$$\frac{\partial^2 p}{\partial x^2} + \frac{\partial^2 p}{\partial y^2} = -\frac{\mu}{k}\frac{q}{h}[\delta(x)\delta(y-d) + \delta(x-d)\delta(y) - \delta(x)\delta(y) - \delta(x-d)\delta(y-d)]$$

$$0 < x < d, 0 < y < d. \tag{4a}$$

Symmetry considerations lead to the adoption of no-flow boundary conditions, i.e. recalling Darcy's law:

$$\left.\frac{\partial p}{\partial x}\right|_{x=0} = \left.\frac{\partial p}{\partial x}\right|_{x=d} = 0 \tag{4b}$$

$$\left.\frac{\partial p}{\partial y}\right|_{y=0} = \left.\frac{\partial p}{\partial y}\right|_{y=d} = 0. \tag{4c}$$

By solving equation (4) one obtains the pressure field, and after applying Darcy's law [equation (3)], the velocity field can be evaluated.

Concentration field

The mass conservation of the tracer may be described as [8]

$$\Phi\frac{\partial C_1}{\partial t} + \nabla\cdot(\mathbf{u}C_1) - \nabla\cdot[\mathbf{K}\nabla C_1] = C_1 Q(x,y) \tag{5}$$

where $\mathbf{K}$ is a diffusion–dispersion tensor, with its complete form given, for example, by Lake [8]. Here, for the sake of simplicity, a diagonal tensor was assumed as

$$K_{xx} = \alpha|u_x| \quad K_{yy} = \alpha|u_y| \quad \text{and} \quad K_{xy} = K_{yx} = 0 \tag{6}$$

where the longitudinal dispersivity constant, α, is a property of the porous medium.

Therefore, equation (5) is rewritten as

$$\Phi\frac{\partial C_1}{\partial t} - \frac{\partial}{\partial x}\left(\alpha|u_x|\frac{\partial C_1}{\partial x}\right) + \frac{\partial}{\partial x}(u_x C_1) - \frac{\partial}{\partial y}\left(\alpha|u_y|\frac{\partial C_1}{\partial y}\right)$$

$$+ \frac{\partial}{\partial y}(u_y C_1) = \frac{q}{h}C_{\text{inj}}[\delta(x)\delta(y-d) + \delta(x-d)\delta(y)]$$

$$-\frac{q}{h}C_1[\delta(x)\delta(y) + \delta(x-d)\delta(y-d)]$$

$$0 < x < d, \quad 0 < y < d, \quad t > 0 \tag{7a}$$

where the concentration being injected at the injection wells has a known prescribed value (equal to C_{inj}).

Assuming that there is initially no tracer within the medium and considering the no-flow boundary conditions, one can state:

$$C_1(x,y,0) = 0 \tag{7b}$$

$$\left.\frac{\partial C_1}{\partial x}\right|_{x=0} = \left.\frac{\partial C_1}{\partial x}\right|_{x=d} = 0 \tag{7c}$$

$$\left.\frac{\partial C_1}{\partial y}\right|_{y=0} = \left.\frac{\partial C_1}{\partial y}\right|_{y=d} = 0. \tag{7d}$$

Equations (7) involve the assumption of continuous tracer injection. The case of slug tracer injection can be solved by superposition or, in a more general form, considering that equation (7) holds for $t < t_{\text{inj}}$, and, after this time, then they hold setting $C_{\text{inj}} = 0$ in equation (7a) and assuming, as an initial condition, the concentration distribution already obtained at $t = t_{\text{inj}}$.

SOLUTION METHODOLOGY

Flow field

System (4) can be solved through conventional analytical methods. Almeida [9] solved it through the classical integral transform technique, obtaining

$$p(x,y) = -\frac{16}{\pi^2}\frac{\mu}{kh}q\sum_{r=0}^{\infty}\sum_{s=0}^{\infty} \times \frac{\cos[(2r+1)(\pi/d)x]\cos[(2s+1)(\pi/d)y]}{(2r+1)^2+(2s+1)^2}. \tag{8}$$

Applying Darcy's law [equation (3)], it then follows that:

$$u_x(x,y) = -\frac{16}{\pi dh}q\sum_{r=0}^{\infty}\sum_{s=0}^{\infty}\frac{(2r+1)}{(2r+1)^2+(2s+1)^2} \times \sin\left[(2r+1)\frac{\pi}{d}x\right]\cos\left[(2s+1)\frac{\pi}{d}y\right] \tag{9a}$$

$$u_y(x,y) = -\frac{16}{\pi dh}q\sum_{r=0}^{\infty}\sum_{s=0}^{\infty}\frac{(2s+1)}{(2r+1)^2+(2s+1)^2} \times \cos\left[(2r+1)\frac{\pi}{d}x\right]\sin\left[(2s+1)\frac{\pi}{d}y\right]. \tag{9b}$$

Expressions (8) and (9) may present a slow convergence behavior. It is possible, however, to improve such convergence [1, 10, 11], though not necessary, since the objective in the present analysis is the solution of the concentration equation, equation (7), not the calculation of the pressure or velocities themselves.

Concentration field

Almeida [9] developed an analytical solution to system (7) through the GITT approach. This procedure is summarized here as follows.

First of all, the steady-state solution is separated to improve the overall convergence behavior, in the form

$$C_1(x,y,t) = C_p(x,y) + C_t(x,y,t) = C_{\text{inj}} + C_t(x,y,t). \tag{10}$$

Substituting equation (10) into equations (7), making use of equation (4a), separating a 'characteristic dispersion' αu_0, and finally rearranging, results in:

$$\frac{\Phi}{\alpha u_0}\frac{\partial C_t}{\partial t}-\frac{\partial^2 C_t}{\partial x^2}-\frac{\partial^2 C_t}{\partial y^2}=$$

$$-\frac{1}{\alpha u_0}\frac{q}{h}C_t[\delta(x)\delta(y)+\delta(x-d)\delta(y-d)]$$

$$+\frac{\partial}{\partial x}\left[\left(\frac{|u_x|}{u_0}-1\right)\frac{\partial C_t}{\partial x}\right]-\frac{1}{\alpha}\frac{\partial}{\partial x}\left[\frac{u_x}{u_0}C_t\right]$$

$$+\frac{\partial}{\partial y}\left[\left(\frac{|u_y|}{u_0}-1\right)\frac{\partial C_t}{\partial y}\right]-\frac{1}{\alpha}\frac{\partial}{\partial y}\left[\frac{u_y}{u_0}C_t\right]. \quad (11)$$

Then, the following auxiliary problems are chosen:

$$\frac{d^2\Psi_i(x)}{dx^2}+\mu_i^2\Psi_i(x)=0 \quad i=0,1,2,3,\ldots \quad (12a)$$

$$\left.\frac{d\Psi_i}{dx}\right|_{x=0}=\left.\frac{d\Psi_i}{dx}\right|_{x=d}=0 \quad (12b)$$

and

$$\frac{d^2\varphi_m(y)}{dy^2}+\lambda_m^2\varphi_m(y)=0 \quad m=0,1,2,3,\ldots \quad (13a)$$

$$\left.\frac{d\varphi_m}{dy}\right|_{y=0}=\left.\frac{d\varphi_m}{dy}\right|_{y=d}=0 \quad (13b)$$

which are readily solved to yield the related eigenfunctions, eigenvalues and norms as $\psi_i(x)=\cos(\mu_i x)$, $\varphi_m(y)=\cos(\lambda_m y)$, $\mu_i=i\pi/d$ $(i=0,1,2,\ldots)$, $\lambda_m=m\pi/d$ $(m=0,1,2,\ldots)$, $N_0=M_0=d$, $N_i=M_m=d/2$ $(i,m\neq 0)$.

Problems (12) and (13) allow for the establishment of the following integral transform pair:

Transform

$$\bar{C}_{im}(t)=\int_0^d\int_0^d\frac{\psi_i(x)}{N_i^{1/2}}\frac{\varphi_m(y)}{M_m^{1/2}}C_t(x,y,t)\,dx\,dy. \quad (14a)$$

Inversion

$$C_t(x,y,t)=\sum_{i=0}^{\infty}\sum_{m=0}^{\infty}\frac{\psi_i(x)}{N_i^{1/2}}\frac{\varphi_m(y)}{M_m^{1/2}}\bar{C}_{im}(t). \quad (14b)$$

Integrating equation (11) over the region $0\leqslant x\leqslant d$, $0\leqslant y\leqslant d$ and $0\leqslant z\leqslant h$, and defining the average potential as

$$C_m(t)=\frac{1}{d^2h}\int_0^h\int_0^d\int_0^d C_t(x,y,t)\,dx\,dy\,dz \quad (15)$$

the differential equation for the average potential is obtained as

$$\frac{dC_m}{dt}=-\frac{2q}{\Phi d^2h}C_t(0,0,t) \quad (16a)$$

$$C_m(0)=-C_{inj}. \quad (16b)$$

Substituting equation (14b) into equation (15), one obtains

$$C_m(t)=\frac{\bar{C}_{00}(t)}{d} \quad (17)$$

that is, the average potential is related to the first transformed potential $\bar{C}_{00}$ $(i=m=0)$ and equation (16) is an independent relation to calculate it.

Then, separating the average potential, i.e. making in equation (11),

$$C_t(x,y,t)=C_m(t)+C(x,y,t) \quad (18)$$

one obtains

$$\frac{\Phi}{\alpha u_0}\frac{\partial C}{\partial t}+\frac{\Phi}{\alpha u_0}\frac{dC_m}{dt}-\frac{\partial^2 C}{\partial x^2}-\frac{\partial^2 C}{\partial y^2}=-\frac{1}{\alpha u_0}$$

$$\times\frac{q}{h}C_m[\delta(x)\delta(y-d)+\delta(x-d)\delta(y)]$$

$$-\frac{1}{\alpha u_0}\frac{q}{h}C[\delta(x)\delta(y)+\delta(x-d)\delta(y-d)]$$

$$+\frac{\partial}{\partial x}\left[\left(\frac{|u_x|}{u_0}-1\right)\frac{\partial C}{\partial x}\right]-\frac{1}{\alpha}\frac{\partial}{\partial x}\left[\frac{u_x}{u_0}C\right]$$

$$+\frac{\partial}{\partial y}\left[\left(\frac{|u_y|}{u_0}-1\right)\frac{\partial C}{\partial y}\right]-\frac{1}{\alpha}\frac{\partial}{\partial y}\left[\frac{u_y}{u_0}C\right] \quad (19a)$$

$$C(x,y,0)=0 \quad (19b)$$

$$\left.\frac{\partial C}{\partial x}\right|_{x=0}=\left.\frac{\partial C}{\partial x}\right|_{x=d}=0 \quad (19c)$$

$$\left.\frac{\partial C}{\partial y}\right|_{y=0}=\left.\frac{\partial C}{\partial y}\right|_{y=d}=0. \quad (19d)$$

Following the formalism [1] in the GITT, we operate the differential equation and the initial condition in system (19) with

$$\int_0^d\int_0^d\frac{\psi_i(x)}{N_i^{1/2}}\frac{\varphi_m(y)}{M_m^{1/2}}dx\,dy$$

and, making use of the auxiliary problems (12) and (13),

$$\frac{\Phi}{\alpha u_0}\frac{d\bar{C}_{im}}{dt}+(\mu_i^2+\lambda_m^2)\bar{C}_{im}=-\frac{1}{\alpha u_0}$$

$$\times\frac{q}{h}\frac{\bar{C}_{00}}{d}\frac{[(-1)^i+(-1)^m]}{N_i^{1/2}M_m^{1/2}}$$

$$-\frac{1}{\alpha u_0}\frac{q}{h}\int_0^d\int_0^d\frac{\psi_i(x)}{N_i^{1/2}}\frac{\varphi_m(y)}{M_m^{1/2}}$$

$$\times[\delta(x)\delta(y)+\delta(x-d)\delta(y-d)]C\,dx\,dy$$

$$+\int_0^d\int_0^d\frac{\psi_i(x)}{N_i^{1/2}}\frac{\varphi_m(y)}{M_m^{1/2}}\frac{\partial}{\partial x}\left[\left(\frac{|u_x|}{u_0}-1\right)\frac{\partial C}{\partial x}\right]dx\,dy$$

$$-\frac{1}{\alpha}\int_0^d\int_0^d\frac{\psi_i(x)}{N_i^{1/2}}\frac{\varphi_m(y)}{M_m^{1/2}}\frac{\partial}{\partial x}\left[\frac{u_x}{u_0}C\right]dx\,dy$$

$$+\int_0^d\int_0^d \frac{\psi_i(x)}{N_i^{1/2}}\frac{\varphi_m(y)}{M_m^{1/2}}\frac{\partial}{\partial y}\left[\left(\frac{|u_y|}{u_0}-1\right)\frac{\partial C}{\partial y}\right]\mathrm{d}x\,\mathrm{d}y$$

$$-\frac{1}{\alpha}\int_0^d\int_0^d \frac{\psi_i(x)}{N_i^{1/2}}\frac{\varphi_m(y)}{M_m^{1/2}}\frac{\partial}{\partial y}\left[\frac{u_y}{u_0}C\right]\mathrm{d}x\,\mathrm{d}y. \quad (20)$$

Substituting the inversion formula (14b) into the integrals of equation (20), an infinite system of coupled linear ordinary differential equations for the transformed potentials, $\bar{C}_{im}$, is obtained. For computational purposes, this system is truncated at the Nth row and column, with N sufficiently large for the required convergence criterion. The truncated system is then written as:

$$\frac{\mathrm{d}\bar{C}_k(t)}{\mathrm{d}t}+\sum_{p=1}^{N} b_{kp}\bar{C}_p(t)=0 \quad (21a)$$

$$\bar{C}_k(0)=-\delta_{1k}C_{\mathrm{inj}}d \quad k=1,2,\ldots,N \quad (21b)$$

where b_{kp} are the elements of the coefficients matrix **B**, as assembled from equation (20) above.

The simplified dispersion tensor allows for the determination of the elements of matrix **B** in closed analytical form [9]; otherwise, numerical quadrature with controlled accuracy should be employed, without any major drawback for employing the present approach.

Following the notation in system (21), each k is associated with a pair (i,m). The inversion formula (14b) is composed of double sums. Instead of truncating both sums in N terms, the double sums are converted into a single sum, taking into account the more representative transformed potentials. It is not possible to know *a priori* how such potentials decay, but it is reasonable to assume that this decay is governed mainly by the functional form $\exp[-(\mu_i^2+\lambda_m^2)t]$, allowing for an ordering scheme based on the values of the sum $(\mu_i^2+\lambda_m^2)$.

It can be shown [9] that, in system (21), only the equations with i and m both even or both odd produce non-zero transformed potentials. Additionally, $\bar{C}_{im}=\bar{C}_{mi}$, which allows for the elimination of redundant equations in system (21).

Since the characteristic velocity, u_0, is not present in the auxiliary problems, it suffices to adopt an average absolute value over the whole domain.

System (21) can be solved analytically [12] as

$$\bar{\mathbf{C}}(t)=\sum_{l=1}^{N}\sigma_l \mathrm{e}^{-v_l t}\boldsymbol{\zeta}^{(l)} \quad (22)$$

where v_l is the lth eigenvalue and $\boldsymbol{\zeta}^{(l)}$ the corresponding eigenvector of matrix **B**. The transformed initial condition (21b) dictates the values of the expansion constants σ_l, as follows,

$$\sum_{l=1}^{N}\sigma_l\boldsymbol{\zeta}^{(l)}=\bar{\mathbf{C}}(0). \quad (23)$$

To determine the eigenvalues v_l, eigenvectors $\boldsymbol{\zeta}^{(l)}$ and coefficients σ_l, specialized routines for matrix eigenvalue problems, like those encountered in the IMSL Library [13], may be used.

The procedure above is related to the continuous tracer injection problem. For tracer slug injection, it can be shown [9] that it suffices, for $t>t_{\mathrm{inj}}$, to recalculate the σ_ls, where the new transformed initial condition is given by $\bar{C}_{1s,k}(0)=\bar{C}_k(t_{\mathrm{inj}})-\bar{C}_k(0)$. Another option is to solve by superposition, i.e. $C_{1s}(x,y,t)=C_1(x,y,t)$ for $t\leqslant t_{\mathrm{inj}}$ and $C_{1s}(x,y,t)=C_1(x,y,t)-C_1(x,y,t-t_{\mathrm{inj}})$ for $t>t_{\mathrm{inj}}$.

Although equations (22) and (23) represent a general solution, for any position within the domain, the practical interest is focused on the effluent concentration profiles (i.e. at the production wells). In this case, it is possible to improve the convergence rates of the eigenfunction expansions by applying an integral balance approach [9], as follows:

$$C_{\mathrm{prod}}(t)=\frac{\Phi h}{2q}d\sum_{l=1}^{N}\sigma_l v_l \mathrm{e}^{-v_l t}\zeta_1^{(l)}. \quad (24)$$

For continuous tracer injection or for tracer slug injection with $t\leqslant t_{\mathrm{inj}}$, C_{inj} must be added to equation (24), according to the separation proposed in equation (10). For tracer slug injection with $t>t_{\mathrm{inj}}$, relation (24) furnishes the concentrations directly.

RESULTS AND DISCUSSION

A literature review indicates that there is no complete analytical solution yet available to problem (7). However, some approximate analytical or purely numerical solutions were identified. Additionally,

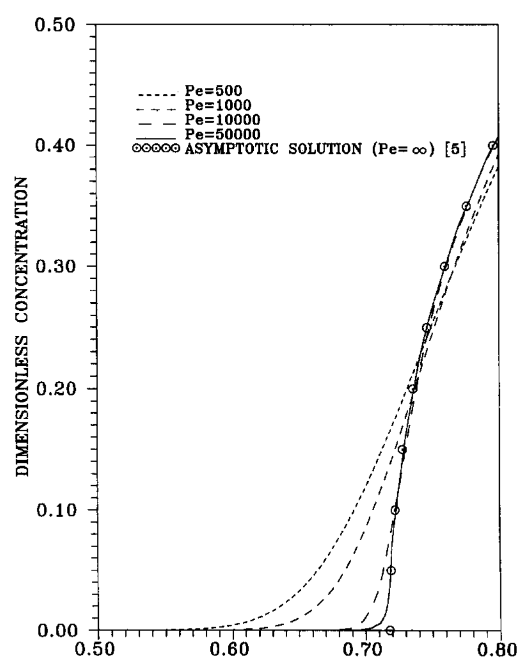

Fig. 2. Comparison of integral transform results, for increasing Peclet number, against asymptotic solution for $Pe=\infty$.

comparisons can be made against asymptotic analytical solutions.

As a first check, the diffusivity α can be reduced successively, leading the present formulation to approach the purely hyperbolic problem, which has a known analytical solution [5]. Figure 2 shows these successive profiles and the comparison with this asymptotic solution. The Peclet number (Pe) relates the convective and the dispersive contributions to the tracer transport and, for this problem, $Pe = a/\alpha$ was adopted as a definition. In Fig. 2, dimensionless concentration $[C_{\mathrm{1D}} = C_1(0,0,t)/C_{\mathrm{inj}} = C_1(d,d,t)/C_{\mathrm{inj}}]$ is plotted against dimensionless time (pore volume injected, $t_{\mathrm{D}} = 2qt/\Phi d^2 h$), and the GITT results show a consistent agreement with the asymptotic solution for $Pe \to \infty$.

Another check is to proceed in the opposite direction, towards the purely diffusive problem, i.e. reducing the Pe number towards zero. The solution for $Pe = 0$ may be obtained through physical argumentation. In this extreme case, all tracer mass introduced via the production wells is immediately uniformly distributed over the whole domain, i.e. the concentration in all points is the same and is only a function of time. Therefore, the definition of the dimensionless average concentration, C_{mD},

$$C_{\mathrm{mD}}(t_{\mathrm{D}}) = t_{\mathrm{D}} - \int_0^{t_{\mathrm{D}}} C_{\mathrm{mD}}(t_{\mathrm{D}})\,\mathrm{d}t_{\mathrm{D}} \quad (25)$$

can be used to solve for $C_{\mathrm{mD}}(t_{\mathrm{D}})$, yielding, for the present initial condition, $C_{\mathrm{mD}}(0) = 0$,

$$C_{\mathrm{mD}}(t_{\mathrm{D}}) = 1 - \mathrm{e}^{-t_{\mathrm{D}}}. \quad (26)$$

Figure 3 shows concentration profiles for sucessively lower Pe and the comparison with solution (26), again with excellent agreement against the integral transform results for very low Peclet number.

The most important approximate analytical solution, to a problem similar to the present one, was developed by Abbaszadeh-Dehghani [5, 6], utilizing a so-called streamlines approach. The dispersion (only longitudinal) was treated in a more rigorous manner than here and various patterns (five-spot included) were studied. Unfortunately, Abbaszadeh-Dehghani's solution furnishes the concentration profiles only in the production wells, for $Pe > 100$ and undefined short tracer slugs. In Fig. 4, the GITT solution (for a 1% tracer slug) is compared with Abbaszadeh-Dehghani's results, for four values of Pe. The concentration is normalized as [5]

$$C_{\mathrm{N}}(t) = \frac{C_{\mathrm{prod}}(t)}{C_{\mathrm{inj}} f_{\mathrm{VP}} \sqrt{Pe}}. \quad (27)$$

Figure 4 shows that the results do not fully coincide, possibly since a simplified dispersion tensor is being considered in the present analysis, but the overall agreement is quite good, indicating that the error

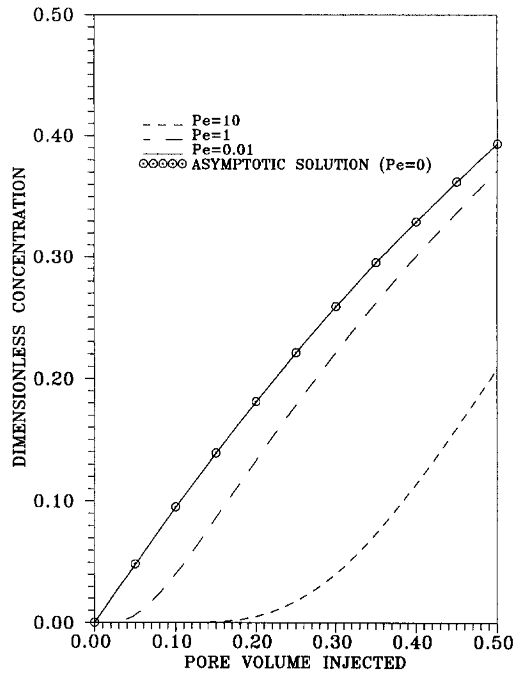

Fig. 3. Comparison of integral transform results, for decreasing Peclet number, against asymptotic solution for $Pe = 0$.

introduced by the simplified tensor is not significant. One can observe that the difference between the two solutions increases as the Peclet number (Pe) is decreased, which was expected, since a lower Pe means a relatively greater importance of the dispersion phenomena.

Now, for comparison purposes with finite difference solutions, two representative schemes were adopted, namely, the nine-point exponential scheme [14, 15] and the third-order TVD scheme with Sweby's region [16, 17]. The calculations were performed with a 15×15 diagonal grid in both cases [9].

Figure 5 shows the behavior of the selected numerical schemes against the GITT solution for $Pe = 500$ and continuous tracer injection. The presence of numerical diffusion in the nine-point exponential scheme and the good agreement with the third-order TVD scheme are clear from this plot. In Fig. 6, a similar comparison is made for $Pe = 100$. In this case, both finite difference schemes results are closer to the present analytical solution, and the numerical diffusion effects are less significant. Table 1 illustrates the convergence behavior of the GITT solution for the continuous tracer injection problem and $Pe = 100$. Table 2 additionally furnishes, for benchmark purposes, the fully converged results for continuous injection, with $Pe = 10$ or $Pe = 500$.

Finally, Fig. 7 compares analytical and numerical concentration profiles along the injection well-production well line for a dimensionless time equivalent to 50% of pore volume injected and various Pe numbers. Table 3 shows the numerical values corresponding to

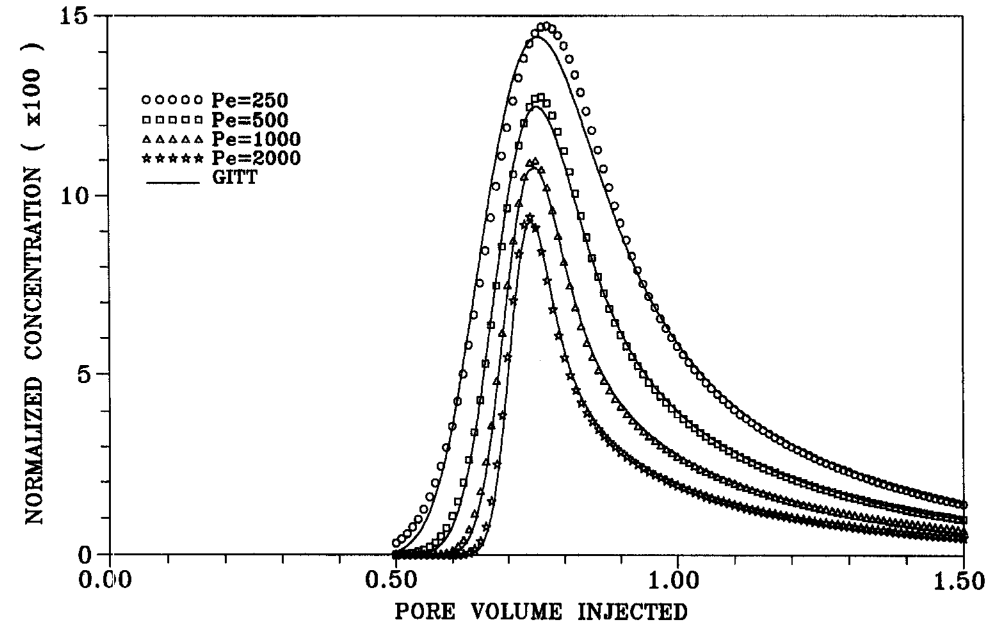

Fig. 4. Comparison of integral transform results, for different *Pe* numbers, against the approximate analytical solution of Abbaszadeh-Dehghani [5, 6].

these profiles. The difficulty of the numerical scheme in perfectly defining the wave front is noticeable in Fig. 7, especially at lower Peclet numbers.

The integral transform approach opens new perspectives in the area of petroleum reservoir engineering. The present application was shown to be quite inexpensive for *Pe* numbers up to 150. For *Pe* numbers higher than 500, the increase in computational cost (CPU time and memory) is, however, justified for benchmark purposes or when accuracy is at a premium. Nevertheless, some techniques for convergence acceleration of the eigenfunction expansions can be employed to alleviate this behavior [10, 11], the most promissing being filtering techniques and the use of a convective auxiliary problem.

Although for this first demonstration of the integral transform method in petroleum reservoir engineering a classical problem with several assumptions was

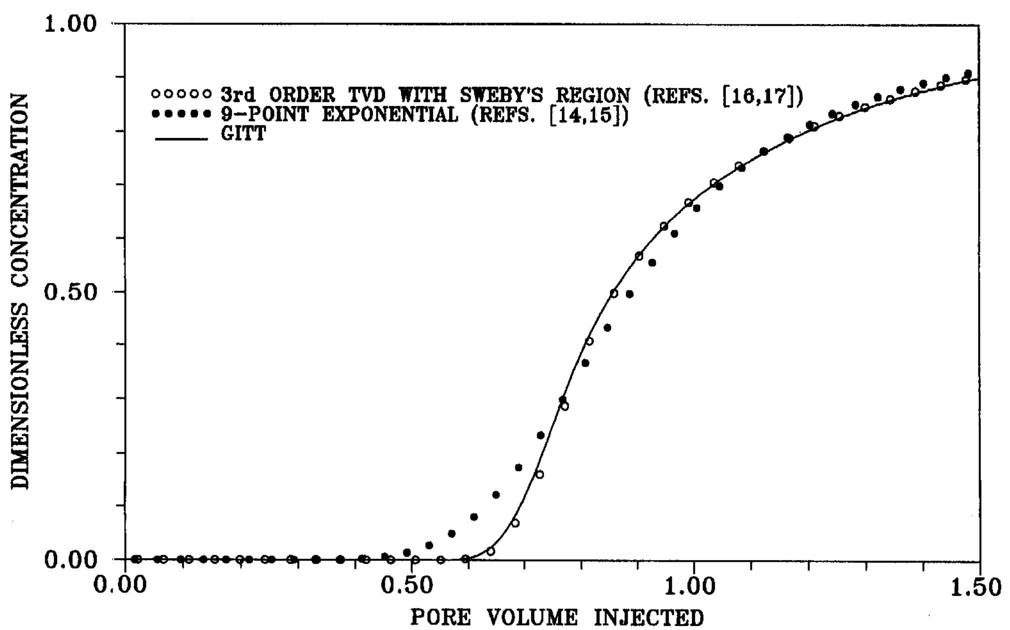

Fig. 5. Comparison of integral transform results against finite difference schemes [14–17], for $Pe = 500$.

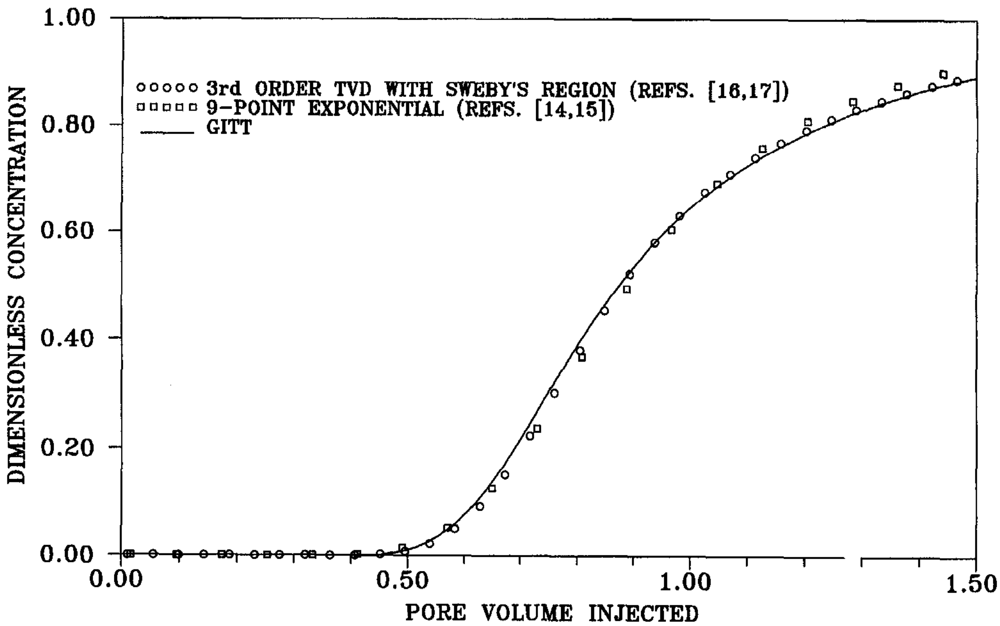

Fig. 6. Comparison of integral transform results against finite difference schemes [14–17], for $Pe = 100$.

Table 1. Convergence behavior of GITT solution for continuous tracer injection and $Pe = 100$

	N						
t_D	20	40	80	160	320	640	1280
0.50	0.019	0.012	0.011	0.011	0.011	0.011	0.011
0.60	0.079	0.075	0.076	0.076	0.076	0.076	0.076
0.70	0.209	0.219	0.218	0.219	0.219	0.219	0.219
0.80	0.380	0.389	0.389	0.389	0.389	0.389	0.389
0.90	0.541	0.535	0.536	0.536	0.536	0.536	0.536
1.00	0.663	0.648	0.647	0.647	0.647	0.647	0.647
1.10	0.740	0.730	0.728	0.728	0.727	0.727	0.727
1.20	0.787	0.787	0.787	0.786	0.786	0.786	0.786
1.30	0.822	0.829	0.831	0.831	0.831	0.831	0.831
1.40	0.858	0.864	0.866	0.865	0.865	0.865	0.865
1.50	0.895	0.894	0.893	0.892	0.892	0.891	0.891

Table 2. Benchmark results for continuous tracer injection and $Pe = 10$ and 500: concentration at the production wells

	Peclet number	
t_D	10	500
0.50	0.209	0.000
0.60	0.308	0.004
0.70	0.403	0.119
0.80	0.488	0.383
0.90	0.563	0.564
1.00	0.628	0.673
1.10	0.683	0.747
1.20	0.729	0.802
1.30	0.769	0.843
1.40	0.802	0.875
1.50	0.831	0.900

Table 3. Benchmark results for continuous tracer injection and $Pe = 10$, 50 and 200: concentration profiles along the line injection well-production well ($t_D = 0.50$)†

Dimensionless position from the injection well	Peclet number		
	10	50	200
0.00	0.986	0.100(1)	0.100(1)
0.10	0.972	0.100(1)	0.100(1)
0.20	0.943	0.100(1)	0.100(1)
0.30	0.887	0.996	0.100(1)
0.40	0.798	0.966	0.100(1)
0.50	0.672	0.843	0.965
0.60	0.522	0.601	0.642
0.70	0.377	0.346	0.190
0.80	0.270	0.174	0.032
0.90	0.217	0.078	0.006
1.00	0.209	0.045	0.001

† Numbers in parentheses indicate powers of 10.

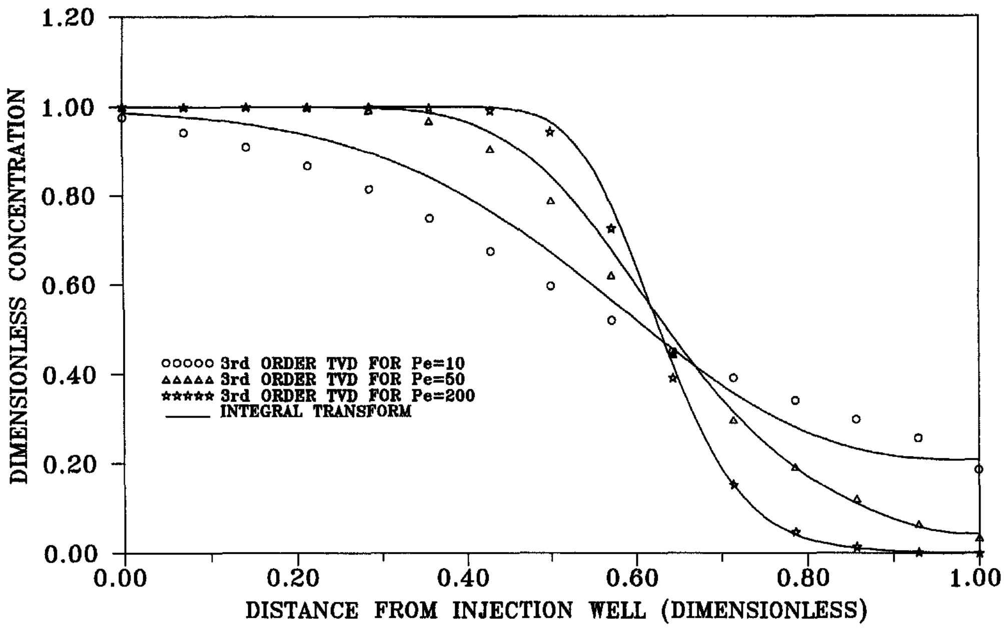

Fig. 7. Comparison of integral transform concentration distributions, for different *Pe* numbers, against the third-order TVD numerical scheme [16, 17].

chosen, there is no major drawback in removing any of them in the context of a practical application.

Acknowledgement—One of the authors (A.R.A.) wishes to acknowledge Petrobras Petróleo Brasileiro S/A for support and permission to publish this paper.

REFERENCES

1. R. M. Cotta, *Integral Transforms in Computational Heat and Fluid Flow*. CRC Press, Boca Raton, Florida (1993).
2. R. M. Cotta, R. Serfaty and R. O. C. Guedes, Integral transform solution of a class of transient convection–diffusion problems, *International Conference on Advanced Computational Methods in Heat Transfer*, Vol. 1, pp. 239–250. Southampton, U.K. (1990).
3. R. Serfaty and R. M. Cotta, Hybrid analysis of transient nonlinear convection–diffusion problems, *Int. J. Numer. Meth. Heat Fluid Flow* **2**, 55–62 (1992).
4. A. J. K. Leiroz and R. M. Cotta, On the solution of nonlinear elliptic convection–diffusion problems through the integral transform method, *Numer. Heat Transfer Part B—Fundamentals* **23**, 401–411 (1993).
5. M. Abbaszadeh-Dehghani, Analysis of unit mobility ratio well-to-well tracer flow to determine reservoir heterogeneity, Ph.D. Thesis, Stanford University, Stanford, CA (1982).
6. M. Abbaszadeh-Dehghani and W. E. Brigham, Analysis of well-to-well tracer flow to determine reservoir layering, *J. Pet. Technol.* **36**, 1753–1762 (1984).
7. S. A. Hovanessian, Pressure studies in bounded reservoirs, *Soc. Pet. Engng J.* **1**, 223–228 (1961).
8. L. W. Lake, *Enhanced Oil Recovery*, Chap. 2. Prentice-Hall, New Jersey (1989).
9. A. R. Almeida, Application of the integral transform technique in petroleum reservoir tracer injection problems, M. S. Thesis (in Portuguese), Universidade Federal do Rio de Janeiro, COPPE/UFRJ, Rio de Janeiro, Brazil (1994).
10. R. M. Cotta, Benchmark results in computational heat and fluid flow: the integral transform method (invited review paper), *Int. J. Heat Mass Transfer* **37**, Suppl. 1, 381–394 (1994).
11. R. M. Cotta, The integral transform method in computational heat and fluid flow (invited keynote lecture), *Tenth International Heat Transfer Conference*. Brighton, vol. 1, pp. 43–60 (1994).
12. W. Boyce and R. DiPrima, *Elementary Differential Equations and Boundary Value Problems* (5th Edn). John Wiley, Singapore (1992).
13. IMSL Library, MATH/LIB, Houston, TX (1987).
14. R. L. A. Santos, Study of the injection of tracers in porous media through the finite differences method with exponential discretization, M.S. Thesis (in Portuguese), Universidade Estadual de Campinas, Campinas, Brazil (1990).
15. R. L. A. Santos, O. A. Pedrosa Jr and A. C. F. Correa, An efficient finite volume approach for modeling miscible displacement, *Second SPE Latin American Petroleum Engineering Conference* (Paper SPE 23691). Caracas, Venezuela (1992).
16. A. C. C. Pinto, High resolution schemes to numerical dispersion control in reservoir simulation, M.S. Thesis (in Portuguese), Universidade Estadual de Campinas, Campinas, Brazil (1991).
17. A. C. C. Pinto, A. C. F. Correa and M. C. C. Cunha, High-resolution schemes for conservation laws: applications to reservoir engineering, *SPE European Petroleum Computer Conference* (Paper SPE 24262). Stavanger, Norway (1982).